

A Non-Invasive Diagnostic Tool for Cardiac Pressure Gradients

Pakorn Wongwaitayakornkul and Muhammad Shamim
Advisors: Matthias Heinkenschloss, Craig Rusin, and Elijah Bolin

2 May 2014

1 Problem Statement

1.1 Introduction

Cardiovascular disease is the leading cause of death in both males and females, and affects people of all ages and races. A wide variety of tools are available to diagnose and treat different cardiac conditions. One particular diagnostic technique involves the measurement of pressure gradients in the heart through a catheter threaded directly to the Atrial and Ventricular chambers of the heart. This project aims to develop an alternative non-invasive technique to measure cardiac pressure gradients and change cardiovascular healthcare.

1.2 Importance

According to the Centers for Disease Control and Prevention, 1 in every 4 deaths in the United States is related to cardiovascular disease. The costs associated with cardiovascular disease, including health care costs and lost productivity, exceed 100 billion dollars in the U.S. alone [VLG⁺11]. Diagnosing and treating cardiovascular disease remains one of the most important aspects of medicine. Furthermore, the only current method of measuring cardiac pressure gradients is an invasive procedure which involves using central line IV access.

1.3 Objective

One diagnostic technique used in treating cardiovascular disease is cardiac pressure measurement within the chambers of the heart. This invasive procedure is administered via a central line and involves the threading of a plastic catheter within the chambers of the heart [Rus13]. Such an invasive procedure can have deadly consequences, including sepsis and death. Our clients, Dr. Craig Rusin and Dr. Elijah Bolin, suggest an alternative non-invasive experimental procedure to measure the pressure gradient. An echocardiogram provides accurate information of the blood flow using the Doppler-shift of the reflected ultrasound wave. The pressure gradient can then be determined from the blood velocity via fluid dynamics equations [Rus13]. The objective is to develop a mathematical model to accurately transform echocardiogram data into pressure gradient information accessible to clinicians.

1.4 Parameter Values

The following parameters are used in the mathematical model. The average human heart rate is 60 bpm. The average viscosity of human blood is $3 - 4 \text{ Pa} \cdot \text{s}$ and the average density of human blood is 1060 kg/m^3 [Ele].

Range of values and units:

blood velocity	cm/s	-56.2 to 56.2
blood density	kg/m ³	1060
blood pressure	mmHg	0 to 150
blood viscosity	Pa · s	3-4
time	s	0 to 1
space	cm	0 to 5

2 Literature Review

2.1 Physiological Background

2.1.1 Anatomy of the Heart

The heart is an organ composed of cardiac muscle cells, responsible for contracting and pumping blood throughout the body. The heart contains four chambers, two atrial chambers and two ventricular chambers [NAE11]. Blood enters the heart from the vena cava through the right atrium and into the right ventricle. The right ventricle contracts to pump the blood into the pulmonary system where oxygen exchange between the lungs and vessels replaces the carbon dioxide in the deoxygenated blood. The oxygenated blood then returns to the left atrium and is pumped into the left ventricle. The left ventricle then contracts to pump blood throughout the body [NAE11].

The synchronized contraction of the various chambers of the heart is controlled by electrical signal conduction. This synchronized signal is sent by a group of cells in the right atrium which form the sinoatrial node. The signal passes through structures of the heart including the atrioventricular node, the bundle branches, and the purkinje fibers. This conduction controls the relative contraction of the different chambers of the heart [NAE11].

2.1.2 Heart Problems and Diagnostic Tools

Any interference with the normal function of the heart can lead to serious medical problems and possibly death. Problems in heart function can be traced to two common sources: electrical conduction problems and physical defects [NAE11]. Electrical conduction problems can result in misaligned contraction of the different heart chambers. Physical defects vary in severity, but generally alter the direction of blood flow through the heart. As such, both of these conditions can result in abnormal heart contractions, and thus ineffective circulation of blood throughout the body [NAE11].

The symptoms of heart disease can manifest in different ways, and modern medicine uses a variety of tools to diagnose heart problems. One of the simplest devices is the electrocardiogram (EKG), a noninvasive technique which measures electrical activity of the heart using topical electrodes. The EKG can detect electrical abnormalities in a waveform and lead to a diagnosis of certain conditions [NAE11].

However, not all heart problems are directly diagnosed using an EKG. Another technique to diagnose problems is the measurement of pressure gradients within the chambers of the heart [YYP86]. As the heart pumps ineffectively in diseased conditions, the flow can be traced to altered pressure gradients in the heart during the contraction cycle (due to a change in the direction of blood flow, weakened contraction forces, etc). To measure the changed cardiac pressure gradients, an invasive procedure is used to thread a catheter through the blood vessels and directly into the chambers of the heart [YYP86]. This catheter then directly measures pressure gradients at the various locations within the cavity, to assist in diagnosing and locating the source of the cardiac problem.

2.1.3 Echocardiograms (Echo)

The alternative treatment that the client proposes depends on the use of echocardiograms. Echocardiograms involve the use of ultrasound wave reflection when interacting with tissues of different density in the human body [AN04]. Doppler wave shifts in the ultrasound can be used noninvasively to obtain different physiological measurements. In the case of continuous-wave Doppler echocardiograms, the focus is on measuring the velocity of blood flow along the length of the ultrasound beam [AN04].

2.2 Mathematical Background

2.2.1 Mathematical Techniques of Previous Software Package

To translate echocardiogram velocity data into pressure gradient information, it is important to understand the physics of blood flow in humans. Daniel J. Penny gives basic physiological information on the ventricular system [Pen99]. Desjardins et al. provide a mathematical framework for using the Navier-Stokes equations to model blood flow [DL99]. Grinberg et al. show numerical simulations of blood flow in arterial networks using 1D and 3D models [LGK10]. Also, by constraining the form of the velocity across the vessel radius, Smith et al. reduce 3D Navier-Stokes equations into 1D problems [NSH02]. Both papers use simplified Navier-Stokes equations with different assumptions.

Most importantly, Yotti et al. present a noninvasive method using color Doppler M-mode (CDMM) image information to measure ejection intraventricular pressure gradients (IVPGs) [RYGF04, RYFA11, RYM05, RYGF05, RYFA07]. Yotti's works were the backbone of the EpiEcho software, developed by the CAAM senior design team in the 2012-2013 academic year.

2.2.2 New Mathematical Approach Literature

This project is a continuation of the EpiEcho CAAM senior design project from 2012-2013 [JHY13]. One of the most challenging aspects of the model is preprocessing the data prior to its analysis for calculating the pressure gradients. The technique of smoothing the spline functions can be found in [Wah90, Rei67].

Another possible method is to smooth the Echo data using Kernel functions and Kernel smoothing. One can apply a density function (usually Gaussian function) onto a noisy point and its neighborhood. The best representation of each noisy point can then be determined from the weighted

average of all the points [WJ95, THF07, LR07, H92].

3 Design Criteria

3.1 Components of Design Criteria

3.1.1 Accuracy

The goal for the project is to develop a potential alternative diagnostic tool for detecting certain cardiac abnormalities. For such a diagnostic tool to be approved by medical authorities, it must be within acceptable accuracy relative to current tools (invasive cardiac catheterization).

3.1.2 Speed

The diagnostic tool must be able to run within a reasonable time frame to allow for timely detection of cardiac abnormalities. It should ideally take less time than current cardiac catheterization procedures. However, the time criterion does not supersede accuracy, as one would rather run code for additional hours and avoid invasive procedures.

3.1.3 User Interface

The majority of medical professionals, including but not limited to echocardiogram technicians and cardiologists, should be able to use the program with minimal training.

3.1.4 Memory/Efficiency

Eventually, the hope is for this program to become an integral component of current echocardiogram machines, and as such, it should be able to run on the machines with their limited memory capacity.

3.1.5 Adaptability for I/O

The solution should be able to handle both images and videos from an echocardiogram.

3.2 Quantification of Design Criteria

3.2.1 Accuracy

Using synchronized echocardiogram and monometer measured physiological data as a metric, the software results should be within an acceptable percent error relative to the catheter data. The exact parameter will be determined by the clinical expert, Dr. Elijah Bolin.

3.2.2 Speed

Invasive cardiac catheterization procedures require much setup and significant time and skill. Creating an alternative non-invasive diagnostic tool is the primary goal. The time requirement is not a major issue, but the program should be completed within a reasonable amount of time, approximately no more than 15–20 minutes on an average laptop.

3.2.3 User Interface

On an ease-of-use scale of 1 (easy) to 5 (hard), a panel of cardiologists and echocardiogram technicians should score the application at 2 or better.

3.2.4 Memory/Efficiency

The program should be able to run on ultrasound machines with limited hardware capabilities.

3.2.5 Adaptability for I/O

The application should be able to use both DICOM pictures as well as DICOM videos.

3.3 Evaluation of Design Criteria

Criteria	Accuracy	Speed	User Interface	Memory Efficiency	Adaptability	Score
Accuracy	-	1	1	1	1	4
Speed	0	-	0	1	1	2
User Interface	0	1	-	1	1	3
Memory/Efficiency	0	0	0	-	0	0
Adaptability for I/O	0	0	0	1	-	1

4 Selected Design Solution

4.1 Mathematical Model

4.1.1 Optimization of the Kernel Matrix

The previous senior design team had developed a solution of preprocessing M Doppler Mode images with spline approximations and then using a simplified Euler form of the Navier-Stokes equation, as shown in equation 1, to solve for the pressure gradient. One potential solution that can be explored is improving the preprocessing of the data using kernel functions rather than relying on spline smoothing.

$$\frac{\partial p}{\partial x} = -\rho \left(\frac{\partial \mathbf{v}}{\partial t} + \mathbf{v} \frac{\partial \mathbf{v}}{\partial x} \right) \quad (1)$$

Different types of Kernel functions can be used depending on the type of smoothing needed and weights assigned to values in the neighborhood of the data point. Some examples include Gaussian, triangular, uniform, and triweight kernel functions.

Kernel functions satisfy the general property

$$\int_{-\infty}^{+\infty} K(u) du = 1 \quad (2)$$
$$K(-u) = K(u) \text{ for all values of } u$$

Blood flow inside the heart is modeled with 1D fluid flow, governed by Burgers' equation (1). Define $v(x, t)$ and $p(x, t)$ as velocity and pressure inside the heart. The two variables are functions of time and space. ν represents the viscosity of the blood and ρ , which is uniform and constant, represents the density of the blood (incompressible fluid). Without loss of generality, it is assumed that $x \in (0, L)$ and $t \in (0, T)$, and the boundary conditions:

$$\begin{aligned} \frac{\partial}{\partial t}v(x, t) - \nu \frac{\partial^2}{\partial x^2}v(x, t) + v(x, t) \frac{\partial}{\partial x}v(x, t) &= \frac{1}{\rho} \frac{\partial p(x, t)}{\partial x} \\ v(0, t) = v(L, t) &= 0 \dots \text{Dirichlet Boundary Condition} \\ v(x, 0) &= v(x, T) \dots \text{Periodicity Condition} \end{aligned} \quad (3)$$

The objective is to find $p(a, t)$ for some $a \in (0, L)$, for any given data $\hat{v}(x, t)$. For simplification, it is assumed that human blood's viscosity is negligible ($\nu \rightarrow 0$). The resulting pressure profile becomes

$$\Pi(\hat{v}, t) = p(a, t) = p(0, t) + \int_{x'=0}^a \left(\frac{\partial}{\partial t} \hat{v}(x', t) + \hat{v}(x', t) \frac{\partial}{\partial x'} \hat{v}(x', t) \right) dx' \quad (4)$$

Problem arises when the velocity data \hat{v} is noisy ($\hat{v} = v_t + \delta v$), where v_t and δv represents the true solution and the noise level respectively. Derivatives on the noisy \hat{v} cause a large error in $\Pi(t)$. To eliminate noise in the data, a Kernel function can be applied to \hat{v} .

A Kernel function is a non-negative real-valued integrable function K with the density function property:

$$\int_0^T \int_0^L K(x, t) dx dt = 1 \quad (5)$$

The Kernel function is confined within a smaller region than the domain, i.e. $K(x - x_0, t - t_0) > 0$ if $(x, t) \in \mathcal{B}(x_0, t_0)$, and $K(x - x_0, t - t_0) = 0$ otherwise. $\mathcal{B}(x_0, t_0)$ defines a confined region in (x, t) -space centered at (x_0, t_0) .

Define the "smoothed" velocity profile as

$$\bar{v}(x, t) = \frac{\int_0^T \int_0^L K(x' - x, t' - t) \hat{v}(x', t') dx' dt'}{\int_0^T \int_0^L K(x' - x, t' - t) dx' dt'} \quad (6)$$

Given the data of the velocity, $\hat{v}(x, t)$, and pressure profile, $\hat{p}(t)$ (measured at $x = a$), an optimization problem can be designed by treating the kernel function as a variable and minimizing the following function:

$$\min_K \Phi(K) = \min_K \int_0^T \|\Pi(\bar{v}, t) - \hat{p}(t)\|^2 dt \quad (7)$$

Particle Swarm Optimization (PSO) was implemented to optimize the Kernel Matrix. Several randomly generated Gaussian matrices were initialized and improved using iterative improvement along perturbation of the Kernel's parameters. The objective function for determining optimality

was the average error when compared to the simultaneous physiological pressure measurements.

Data: K_i is the Kernel Matrix, P_i is resulting pressure gradient, P_A is the actual pressure gradient from physiological data, e_i is the error between P_i and P_A

Result: \hat{K} Optimized Kernel Matrix

for $i = 0:n$ **do**

 Random Initialization of K_i ;

$P_i \leftarrow$ Run code with K_i and obtain resulting pressure gradient;

$e_i \leftarrow$ Error(P_i, P_A);

end

$\hat{i} \leftarrow$ argmin(e_i);

$\hat{K} \leftarrow K_{\hat{i}}$;

$\hat{e} \leftarrow e_{\hat{i}}$;

while $\hat{e} >$ (*tolerance*) **do**

for $i = 0:n$ **do**

$M_i \leftarrow$ perturbation of K_i ;

$R_i \leftarrow$ Run code with M_i and obtain resulting pressure gradient;

if Error(R_i, P_A) $<$ e_i **then**

$K_i \leftarrow M_i$;

$e_i \leftarrow$ Error(R_i, P_A);

if $e_i <$ \hat{e} **then**

$\hat{K} \leftarrow K_i$;

$\hat{e} \leftarrow e_i$;

end

end

end

end

Algorithm 1: PSO Algorithm to Optimize Kernel Matrix

4.1.2 Solving 1D Euler Momentum Equation using Optimization

The previous senior design team used specific assumptions regarding the Navier-Stokes equation, based on the model used by Yotti et al [RYGF04], which involved spline smoothing the preprocessing data. However this approach does not provide a rigorous physical meaning in the process of smoothing the data. Another viable solution is to solve the 1D Euler Momentum Equation using optimization of the linear system. In this way, the data used can be noisy and the problem can be solved by a mathematical approach that makes sense physically.

Dr. Heinkenschloss' codes were adapted to solve this problem [Hei]. The problem is as followed:

Minimize

$$\min_u \frac{1}{2} \int_0^T \int_0^1 (y(x, t) - z(x, t))^2 + \omega u^2(x, t) dx dt, \quad (8)$$

where y is the solution of

$$\begin{aligned}
\frac{\partial}{\partial t}y(x, t) - \nu \frac{\partial^2}{\partial x^2}y(x, t) + \frac{\partial}{\partial x}y(x, t)y(x, t) &= r(x, t) + u(x, t) & (x, t) \in (0, 1) \times (0, T), \\
y(0, t) = y(1, t) &= 0 & t \in (0, T), \\
y(x, 0) &= y_0(x) & x \in (0, 1),
\end{aligned} \tag{9}$$

where $z : (0, 1) \times (0, T) \rightarrow \mathbb{R}$, $r : (0, 1) \times (0, T) \rightarrow \mathbb{R}$, and $y_0 : (0, 1) \rightarrow \mathbb{R}$ are given functions and $\omega, \nu > 0$ are given parameters. $\nu > 0$ is also a parameter, representing the viscosity of the blood.

4.2 Implementation

4.2.1 Experimental Data

On 2/20/2014, a clinical experiment was conducted at Texas Children's Hospital (TCH) with Dr. Elijah Bolin. Dr. Craig Rusin and Pakorn Wongwaitayakornkul were also in attendance. Physiological measurements were gathered during the experiment from a 8.71 kg baby pig. During the experiment, a fluid filled catheter and micromonometer were threaded into the base of the right atrium and apex of the right ventricle. Simultaneous to these pressure measurements, Motion Doppler Mode Echocardiograms were obtained. Additional measurements were obtained under simulated conditions of hypertension, hypotension, and hypoxia via epinephrine administration, esmolol administration, and decreased oxygen administration respectively.



Figure 1: Image of the Operation

4.2.2 Procedure

For the kernel smoothing approach, DICOM images were obtained from the echocardiogram and converted to a velocity profile as shown in Figure 2. The velocity data was de-noised using a Kernel Matrix. Given the smooth velocity profile, the pressure gradient was then obtained using the 1D Euler Momentum Equation. Spatial integration was then used to obtain the pressure curve. PSO was used to perturb the Kernel Matrix $K(x, t)$ to minimize the error in matching the pressure as described in section 4.1.1.

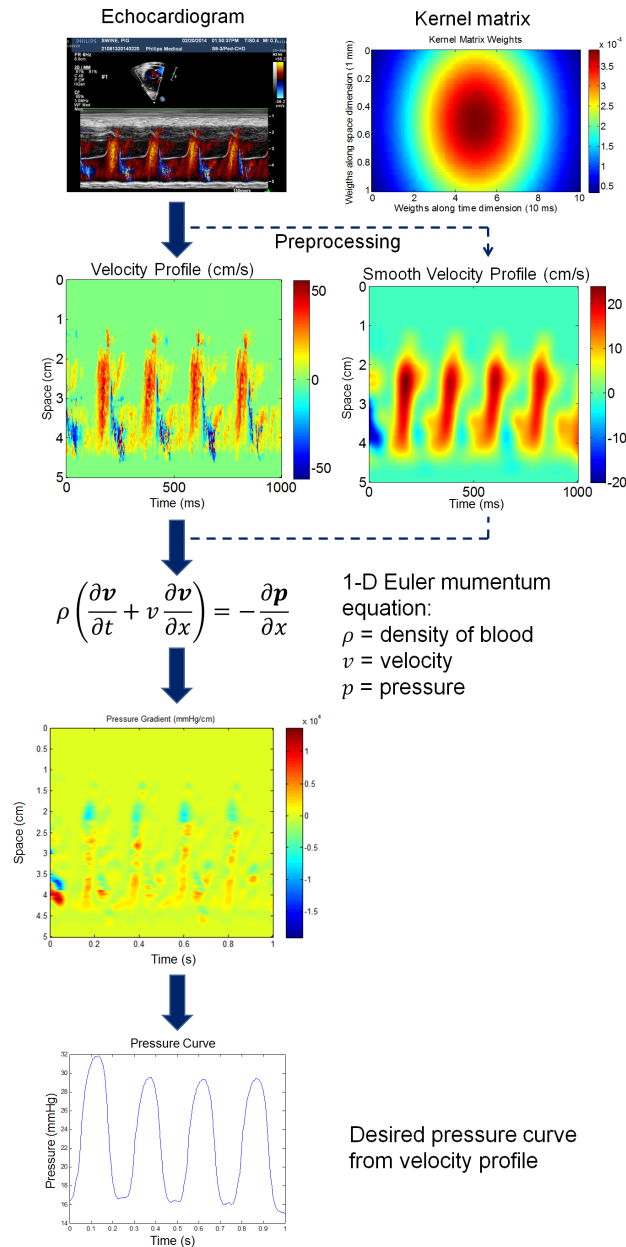


Figure 2: Flowchart of the Procedure

4.2.3 Synthesized Data

Unfortunately, the calculated pressure gradient from the mathematical model bore little resemblance in scale or shape to the physiological data obtained from the pig lab. Therefore, validity of the Kernel Matrix Optimization by PSO was verified on a synthesized data set, illustrated in Figure 3. Due to the difficult nature of exploring unrestrained Kernel Matrices with their high degree of freedom, the optimization was restricted to optimizing Gaussian Kernel Matrices with three variable parameters (p, q, σ) . The Gaussian Kernel Matrix size was p by q and its standard deviation was σ .

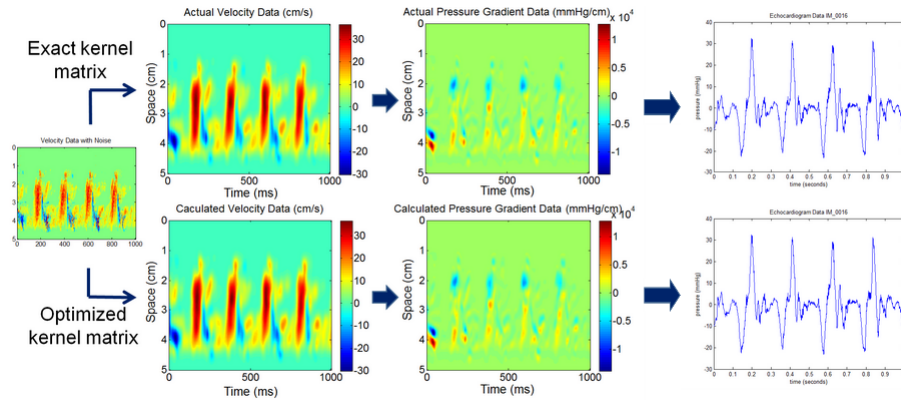


Figure 3: Illustration of Data Synthesis: (Left) Velocity data with noise
 (Top Row) Synthesized data assumed as exact physiological
 measurements (Bottom Row) Recovered data after optimized Kernel
 smoothing to eliminate noise

5 Obstacles

As mentioned above, a significant disagreement was encountered in the pressure curve calculated from the mathematical model and the physiological data obtained at TCH, demonstrated in Figure 4. The amplitude differs by a factor of 3.3 with additional differences in the shape of the waveform. It is important to note that the change in pressure is of clinical significance as the offset varies by initial pressure conditions.

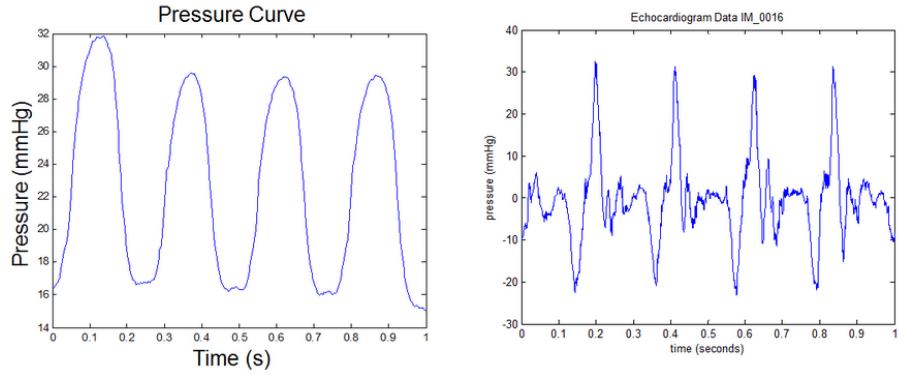


Figure 4: Disagreement of Pressure Curve: (Left) Pressure measured from catheter (Right) Corresponding pressure output from mathematical model

6 Results

Using PSO optimization, convergence was obtained for optimization of the Kernel Matrix on synthesized data. Figure 5 demonstrates the paths of 10 particles (different initial Kernel Matrices), as they converged onto the optimal matrix (red dot).

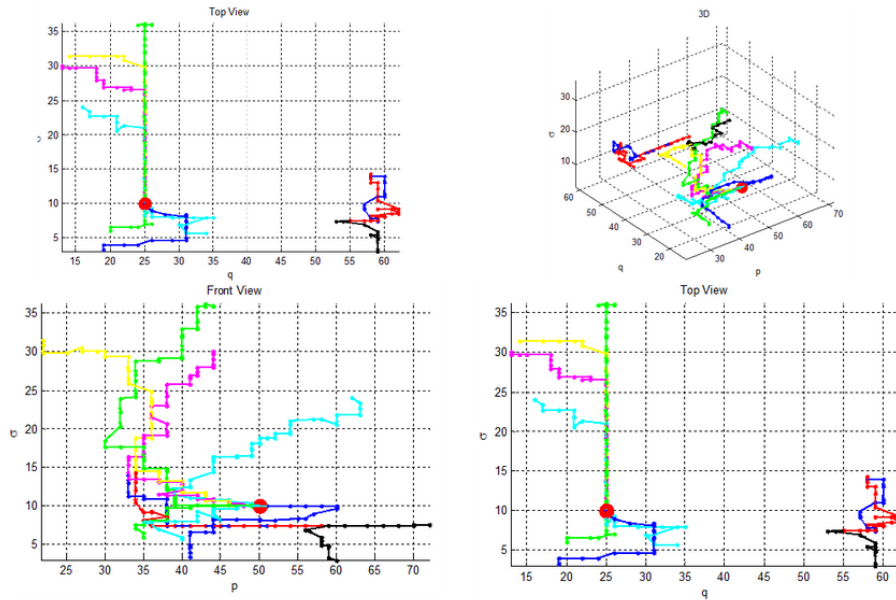


Figure 5: Convergence Path of Particles in PSO

Figure 6 shows the relative error for each particle decreasing over time. For the plot given in Figure 6, 7 out of 10 initial particle seem converge within 300 iterations, while 3 remain stuck in a local optimum.

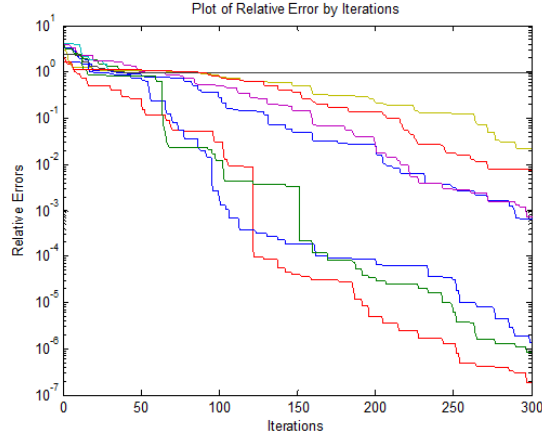


Figure 6: Convergence Obtained with PSO

7 Future Work

There are currently major concerns regarding the validity of the 1D Euler Momentum Equation being applied to the calculation of cardiac pressure gradients. The original support for this approach came from research by Yotti, et al [RYM05]. However, the implementation of the 1D Euler Momentum Equation by the previous senior design team, and verified by the current team, outputs data significantly different in shape and scale from the physiological data measured in the pig lab.

The implementation of the 1D Euler Momentum Equation appears valid, and as such, the concern is in the appropriateness of applying the simplified model to the original problem of calculating cardiac pressure gradients. Two potential routes exist. There may be relatively simple scaling issues to fix in the 1D Euler Momentum implementation. If so, the next step would simply involve fixing these scaling errors and running the current verification model with the obtained physiological data. Otherwise, it is necessary to revise the original mathematical model and consider alternative approaches.

8 Conclusion

Cardiovascular disease is one of the leading causes of death around the world and affects people of all ages and races. Several diagnostic tools are used by cardiologists to diagnose and treat cardiovascular problems, including the measuring of cardiac pressure gradients. Current methods require invasive catheters threaded directly to the chambers of the heart for accurate pressure measurements. This project has focused on developing a non-invasive alternative to measuring these gradients using the 1D Euler Momentum Equation applied to Motion-Mode Echocardiograms.

The solution involved building on software developed by a previous senior design team and eliminating noise from the velocity profile using an optimized set of Kernel Matrices. PSO was implemented to optimize the size and standard deviation of a Gaussian Kernel Matrix, and successfully tested on synthetic data to eliminate noise in the velocity data. Physiological baby pig data was obtained from TCH. However, the discrepancies between the output from the mathematical model and the

physiological data suggest that the mathematical model may not be appropriate for recovering cardiac pressure gradients, or may require recalibration.

References

- [AN04] Euan A Ashley and Josef Niebauer. *Cardiology: Explained*. Remedica, 2004.
- [DL99] Benoit Desjardins and Chi-Kun Lin. A survey of the compressible navier-stokes equations. *Taiwanese Journal of Mathematics*, 3(2), 1999.
- [Ele] Glenn Elert. Viscosity. *The Physics Hypertextbook*.
- [H92] Wolfgang Härdle. *Applied Nonparametric Regression*. Cambridge University Press, 1992.
- [Hei] Matthias Heinkenschloss. Numerical solution of implicitly constrained optimization problems. Technical report, Rice University.
- [JHY13] Andrew Tilley Joey Huchette, Hrothgar and Guang Yang. Caam 496 senior design final report. 2013.
- [LGK10] T. Anor J. Madsen L. Grinberg, E. Cheever and G. Karniadakis. Modeling blood flow circulation in intracranial arterial networks: A comparative 3d/1d simulation study. *Annual of Biomedical Engineering*, 51:1035–1042, 2010.
- [LR07] Q. Li and J.S. Racine. *Nonparametric Econometrics: Theory and Practice*. Princeton University Press, 2007.
- [NAE11] NAEMT. *Advanced Medical Life Support*. Jones & Bartlett Learning, 2011.
- [NSH02] A. Pullan N. Smith and P. Hunter. An anatomically based model of transient coronary blood flow in the heart. *SIAM Journal of Applied Mathematics*, 62, 2002.
- [Pen99] Daniel J Penny. The basics of ventricular function. *Cardiology in the Young*, 9(02):210–223, 1999.
- [Rei67] C. H. Reinsch. Smoothing by spline functions. *Numerische Mathematik*, 10, 1967.
- [Rus13] Dr. Craig Rusin. Cardiac pressure gradient project meeting. Texas Children’s Hospital, October 2013.
- [RYFA07] M. M. Desco J. C. Antoranz-J. L. Rojo-Alvarez C. Cortina D. Garcia M. Moreno-M. A. Garcia-Fernandez R. Yotti, J. Bermejo and F. Fernandez-Aviles. Noninvasive assessment of the right ventricular filling pressure gradient. *Circulation*, 116, 2007.
- [RYFA11] Y. Benito J. Antoranz M. Desco-D. Rodriguez-Perez-C. Cortina T. Mombiela A. Barrio J. Elizaga R. Yotti, J. Bermejo and F. Fernandez-Aviles. Noninvasive estimation of the rate of relaxation by the analysis of intraventricular pressure gradients, cardiovascular imaging. *Journal of the American Heart Association*, 2011.
- [RYGF04] J. C. Antoranz J. L. Rojo-Alvarez C. Allue-J. Silva M. M. Desco M. Moreno R. Yotti, J. Bermejo and M. A. Garcia-Fernandez. Noninvasive assessment of ejection intraventricular pressure gradients. *Journal of the American College of Cardiology*, 43, 2004.

- [RYGF05] M. M. Desco J. C. Antoranz-J. L. Rojo-Alvarez C. Cortina C. Allue H. Rodriguez-Abella M. Moreno R. Yotti, J. Bermejo and M. A. Garcia-Fernandez. Doppler-derived ejection intraventricular pressure gradients provide a reliable assessment of left ventricular systolic chamber function. *Circulation*, 112, 2005.
- [RYM05] M. M. Desco J. C. Antoranz-J. L. Rojo-Alvarez C. Cortina C. Allue L. Martin-M. Moreno M. A. Garcia-Fernandez J. Serrano R. Yotti, J. Bermejo and R. Munoz. A noninvasive method for assessing impaired diastolic suction in patients with dilated cardiomyopathy. *Journal of the American Heart Association*, 112, 2005.
- [THF07] R. Tibshirani T. Hastie and J. Friedman. *The Elements of Statistical Learning*. Springer, 2007.
- [VLG⁺11] Amy L Valderrama, Fleetwood Loustalot, Cathleen Gillespie, Mary G George, and MPH Schooley. Million hearts: Strategies to reduce the prevalence of leading cardiovascular disease risk factors- united states, 2011. *Morbidity and Mortality Weekly Report*, 60(36), 2011.
- [Wah90] G. Wahba. Spline models for observational data. *Society for Industrial and Applied Mathematics*, 1990.
- [WJ95] M. P. Wand and M. C. Jones. *Kernel Smoothing*. London, New York : Chapman & Hall, 1995.
- [YYP86] Mark Yeager, Paul G Yock, and Richard L Popp. Comparison of doppler-derived pressure gradient to that determined at cardiac catheterization in adults with aortic valve stenosis: Implications for management. *The American Journal of Cardiology*, 57(8):644–648, 1986.